Metrol. Meas. Syst., Vol. XXII (2015), No. 4, pp. 565–576.

PAN POLSKA AKADEMIA NAUK

METROLOGY AND MEASUREMENT SYSTEMS

Index 330930, ISSN 0860-8229
www.metrology.pg.gda.pl

M&MS

LARGE AREA CONCRETE SURFACE TOPOGRAPHY MEASUREMENTS USING OPTICAL 3D SCANNER

Radomir Majchrowski[1)], Mirosław Grzelka[1)], Michał Wieczorowski[1)], Łukasz Sadowski[2)], Bartosz Gapiński[1)]

1) Poznan University of Technology, Faculty of Mechanical Engineering and Management, Piotrowo 3, 60-965 Poznań, Poland (Radomir.Majchrowski@interia.pl, Miroslaw.Grzelka@put.poznan.pl, Michal.Wieczorowski@put.poznan.pl, Bartosz.Gapinski@put.poznan.pl)

2) Wroclaw University of Technology, Faculty of Civil Engineering, Wybrzeże Wyspiańskiego 27, 50-370 Wrocław, Poland (✉ lukasz.sadowski@pwr.edu.pl, +48 505 901 069)

Abstract

The paper presents examinations of the surface of base concrete with a 3D scanner. Two base concrete surfaces, differently prepared, were examined, together with two measurement strategies: simple and fast 3D scanning and partial scanning in selected areas corresponding to the device measurement space. In order to complete the analysis of a concrete surface topography an original Matlab-based program TAS (*Topography Analysis and Simulation*) was developed for both 2D and 3D surface analyses. It enables data processing, calculation of parameters, data visualization and digital filtration.

Keywords: 3D surface metrology, concrete, optical method, roughness, topography measurement.

1. Introduction

Concrete multilayer elements have become increasingly popular in residential buildings and multi-level garages [1–2] owing mainly to their durability in comparison with other types [3]. Unfortunately, construction defects, such as lack of adhesion between the base concrete layer and the topping, reduce this durability [4–14].

An attempt to determine a correlation between concrete surface roughness parameters and the degree of bonding is described in [15], where it is shown that there is a correlation between concrete surface roughness parameters and the resistance of concrete layers to delamination, measured by the semi-destructive (SDT) pull-off method. Garbacz *et al.* [16] analysed correlations between the concrete surface geometry parameters determined by laser profilometry, mechanical profilometry, the microscopic method and the "sand" (macroscopic) method as well as correlations between the parameters and the adhesion of layered concrete members. Davis [17] and Hertlein [18] recommend the non-destructive impulse response (IR) method to search for delamination in concrete layers. They successfully applied the IR method to small area concrete surfaces. Franck and De Belie [19] analysed the impact of concrete surface roughness on a bovine claw model and deformation of the latter under load. The roughness parameters were determined by the profile method using a high-precision laser beam. Because, as defined in [20], concrete is a composite material composed of a coarse granular material (aggregate or filler) embedded in a hard matrix (cement or binder) which fills the space between the aggregate particles and glues them together, a surface profile analysis can miss important information (Fig. 1). It is worth noting that a single profile does not sufficiently characterize surface properties. In [21–22] the authors attempted to carry out a 3D analysis

Article history: received on Apr. 04, 2015; accepted on Aug. 24, 2015; available online on Dec. 07, 2015; DOI: 10.1515/mms-2015-0046.

of the surface of concrete, but the methodology used made it possible to measure only a very small part of the analysed surface.

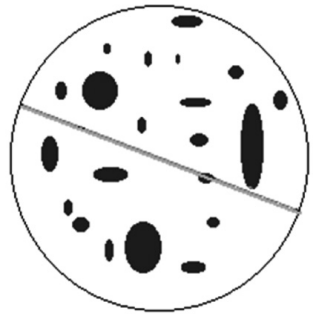

Fig. 1. A profile measurement or a measurement of surface topography.

Therefore, a methodology for measuring and analysing the surface topography of a large area of concrete at high resolution needs to be developed [23]. It is also important to determine which 3D parameters best describe the topography of concrete.

2. Materials and methods

2.1. Coordinate measurement technique

In mechanical engineering surface measurements were initially associated with the measurement of a surface profile (2D measurement). Even today 2D measurements are still used, especially in industry. Unfortunately, this type of measurement has serious limitations, shown in Fig. 1. In the last decades many scientists and designers have become convinced that the third dimension should be added to the analysis [24–35]. Today the 3D analysis of surface geometry has become widely accepted, though there is still some disorder in the terminology and classification of 3D parameters. Various methods are used to measure the surface topography [36–38]. Most of the existing topography analysis systems are based on a number of profiles, mostly parallel [39, 40]. Myshkin [41] proposed the following division of measuring methods: stylus methods, optical methods, SEM methods, AFM and STM methods. A similar, but more detailed division is shown in [24]. The above methods can be used to measure areas from nm to mm in size, which is not sufficient for the proper measurement of concrete surface topography. Therefore, a nonstandard method of measuring the concrete surface topography is needed. In the case of large concrete surface details, the measured points of an inspected feature are usually distant from each other. The best solution seems to be an optical method combined with the coordinate measurement technique [42–45]. There are several optical methods of measuring the coordinates of 3D objects. They are generally divided into active and passive methods. The coordinate measuring scanner used in the research (Fig. 2a) is a stereoscopic system based on two measuring cameras.

The scanner uses the *digital light projection* (DLP) method and is equipped with measuring objectives (corresponding to certain measured spaces) and a high-quality projector ensuring a very high resolution of the cloud of points. Using this scanner one can scan elements from a few millimetres to a few tens of meters in size. The scanner measurement method is based on the principle of triangulation (Fig. 2b), consisting in observing the pattern of spectral lines on the measured detail by two cameras and then calculating a coordinate point for each camera pixel.

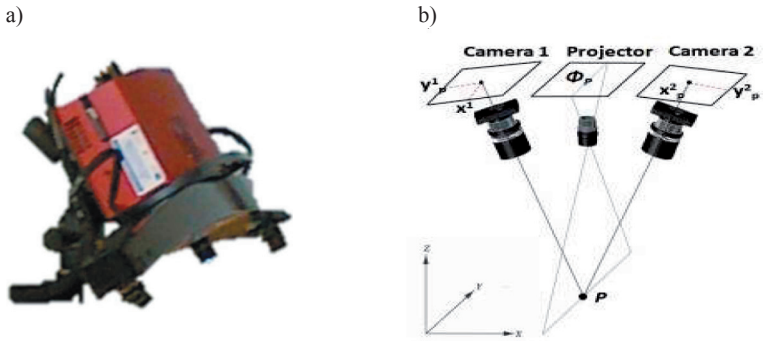

Fig. 2. A coordinate measuring 3D scanner GOM ATOS II: a) a measuring camera; b) the principle of triangulation.

The measurement area of the optical scanner may vary from 175 x 140 to 2000 x 1600 [mm^2] and its declared resolution is 20 μm in all directions (x, y, z). The accuracy of identifying the points depends on the measurement area, the distance between single probing points, the method of measurement responsible for registration of the cloud of points corresponding to the measured object, and on the data processing method [25]. The dimensions of concrete surfaces sometimes exceed 10000 mm and then they can be considered as large scale details. In order to measure such details one can use one of the following proper measurement strategies ensuring the required accuracy of the measurement results [43]:

– Measurement Strategy A: simple and fast 3D scanning; the measured detail is placed within the measurement area of the optical coordinate system; the detail can be slightly larger (Fig. 3a).
– Measurement Strategy B: the measured detail is subjected to partial scanning (in selected areas corresponding to the device measurement space) until all data are acquired. As opposed to Measurement Strategy A, the complete scanning of a detail is possible here only by performing a series of single measurements (Fig. 3b).

The accuracy of identifying the particular points depends directly on the measured space, the distance between single probing points, the measurement method responsible for registration of the cloud of points corresponding to the measured object (Fig. 4a), and on the method of data processing in the polygonization process necessary to transform the cloud of points into a virtual object defined by a polygonal grid of triangles (Fig. 4b) [43].

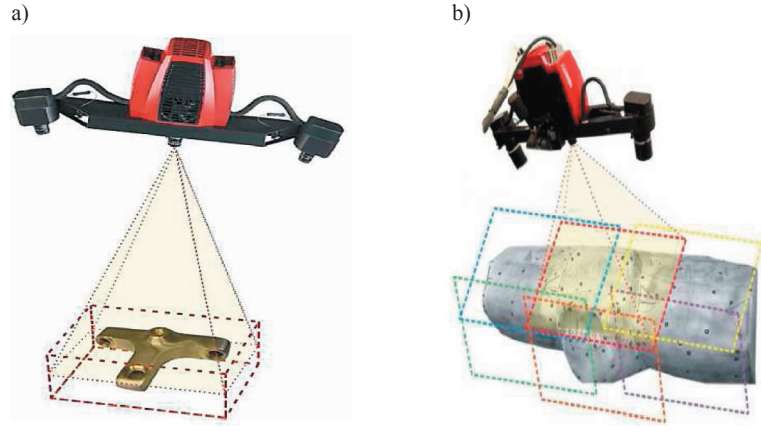

Fig. 3. a) Measurement Strategy A; b) measurement Strategy B [42].

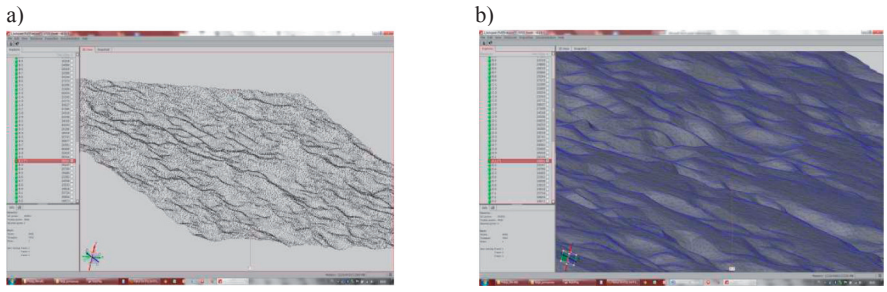

Fig. 4. a) The cloud of points corresponding to the measured detail; b) a grid of triangles after the polygonization process.

2.2. TAS software

In order to complete the analysis of a concrete surface topography, our team has developed an original Matlab-based program for both 2D and 3D surface analyses. The program is called TAS (*Topography Analysis and Simulation*). It includes four modules: an initial data processing module, a basic parameter calculating module, a data visualization module and a digital filtration module. The latter is a Gaussian filter designed in accordance with the draft standard ISO/TC 213 N510 recommendations and described by (1):

$$h(x,y)=\frac{1}{\beta\lambda_{xc}\lambda_{yc}}\exp\left\{-\frac{\pi}{\beta}\left[\left(\frac{x}{\lambda_{xc}}\right)^2+\left(\frac{y}{\lambda_{yc}}\right)^2\right]\right\}. \tag{1}$$

Examples of filtration are shown in Fig. 5.

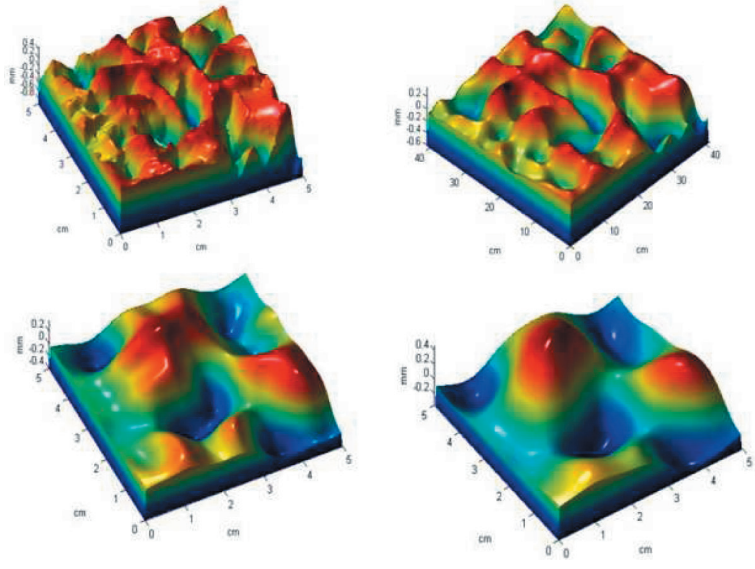

Fig. 5. Examples of Gaussian digital filtration: impulse responses and concrete surfaces.

An algorithm has been developed to calculate 3D surface topography parameters. According to Stout *et al.* [27] the 3D parameters can be divided into four groups: amplitude, spatial, hybrid and functional ones. The amplitude and functional parameters are most useful for evaluation of

a concrete surface topography. In most cases it is enough to use eight parameters [27–34]. In order to distinguish the parameters acquired from the surface from those determined on the basis of a single profile the former ones are marked with the letter S.

2.3. Experimental setup

Two 125 mm thick 2500x2500 mm large area concrete surfaces were examined. The concrete surfaces were made of class C30/37 concrete with a maximum aggregate grading of 8 mm. The surfaces were laid on a 2 mm thick polyethylene sheeting and a 100 mm thick sand layer. The surfaces were cured naturally in a laboratory hall (air temperature of +18°C, relative air humidity of 60%). During the first week they were stored under sheeting. Concrete surface I was prepared by mechanical grinding while surface II after concreting was not prepared (after concreting the surface was left unchanged).

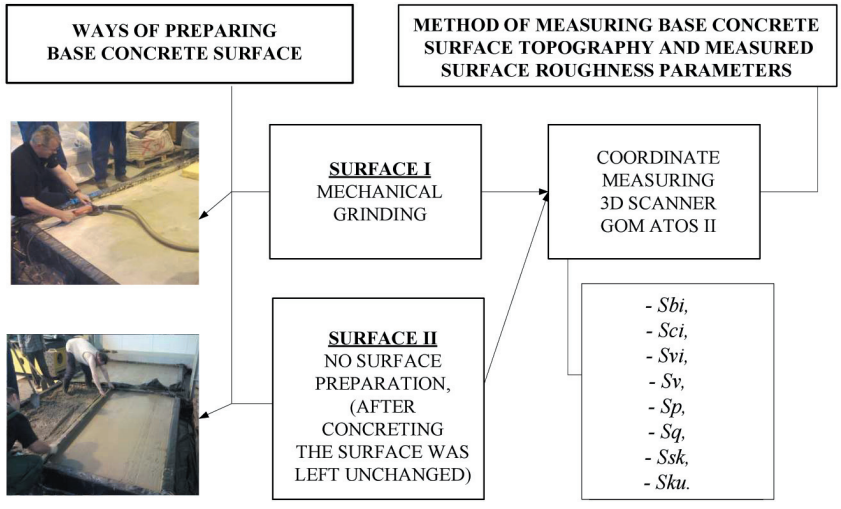

Fig. 6. The ways of preparing the base concrete surface, the methods of measuring its topography and the measured surface roughness parameters.

Figure 6 shows the ways of preparing the base concrete surfaces, the method of measuring the base concrete surface topography and the measured surface roughness parameters.

The scanner maximum measurement horizontal range of 2000 x 1600 [mm^2] was used in this study. The area of the concrete surfaces was divided into several smaller areas. After the concrete slabs had been labelled a 1500 x 1500 mm test area was demarcated on each of them. A grid of points spaced at every 100 mm was marked on each of the slabs. The columns were denoted with letters from A to H and the rows were numbered from 1 to 16. In total, 256 measured points were marked on each surface (Fig. 7).

The entire surface of the slab was scanned by the optical scanner (Fig. 8) and then – using the dedicated software – a 3D image of the scanned surface was obtained.

In order to determine 3D parameters of the examined concrete surfaces, it became necessary to develop an algorithm for processing the measurement data. The surface scanning yielded a cloud of points. To convert the points onto a rectangular grid the Matlab's "griddata function" was used. This function fits a surface in the form z = f (x, y) to data in nonuniformly spaced vectors (x, y, z). The griddata function interpolates the surface at the points specified by (Xi, Yi) to produce Zi. The surface always passes through data points Xi and Yi, forming a uniform grid (Fig. 9).

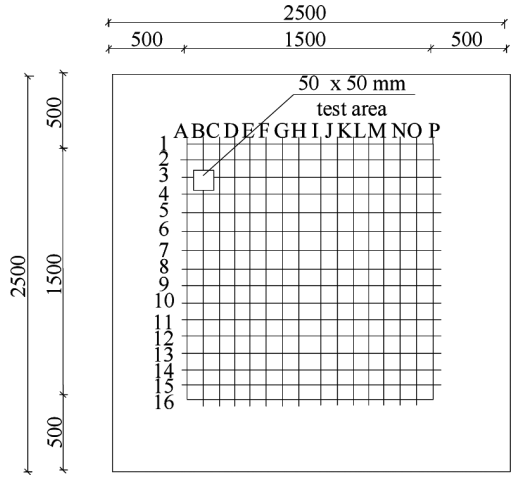

Fig. 7. Distribution of measured points on the examined concrete slabs.

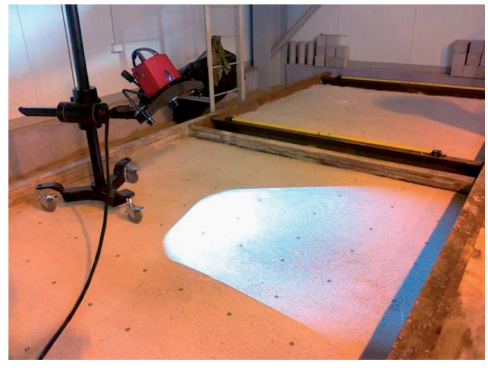

Fig. 8. Scanning a concrete surface with the optical coordinate measuring scanner.

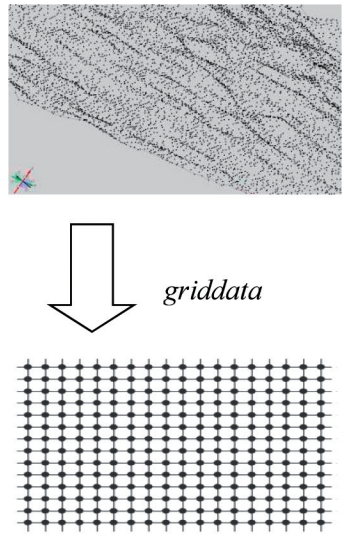

Fig. 9. The cloud of points converted onto a rectangular grid.

3. Results and discussion

The numerical values of the particular base concrete surface roughness parameters in each measured point were determined. Examples of the obtained surface topography images for a selected point on surface I and II are presented below (Figs. 10–13).

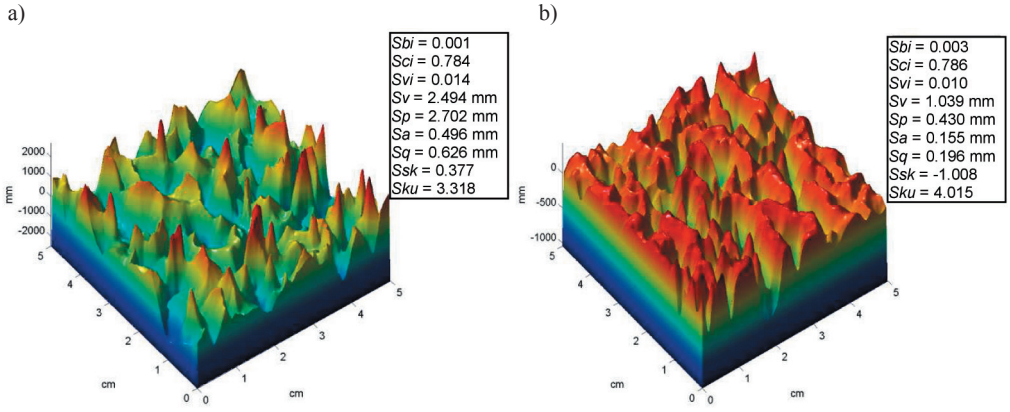

Fig. 10. Examples of the obtained surface topography images for a selected point A1: a) surface I; b) surface II.

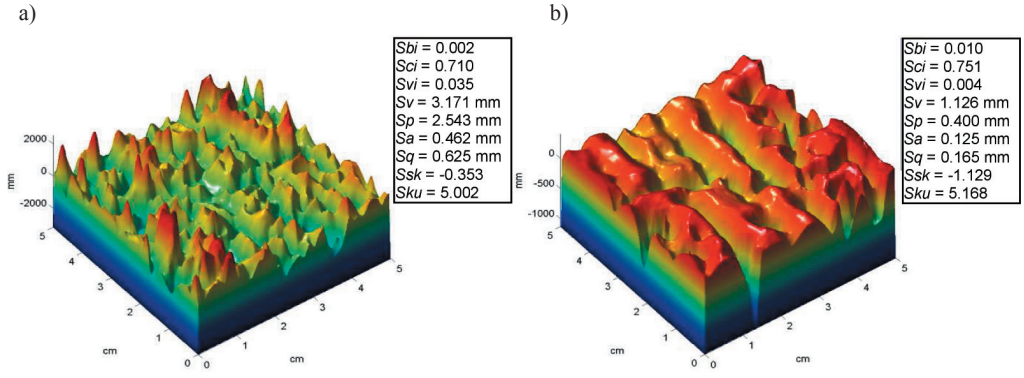

Fig. 11. Examples of the obtained surfaces topography images for a selected point C6: a) surface I; b) surface II.

After scanning the concrete surfaces 80 areas for each of the analysed concrete slabs were obtained. For each of the surfaces their 3D topography parameters (amplitude parameters, spatial parameters, hybrid parameters and functional parameters) were calculated using the TAS software. Then, the average values of 256 parameters and the mean deviations were calculated. Fig. 14a shows an example of the *Ssk* amplitude parameter distribution calculated for concrete surface number II while Fig. 14b shows an example of the *Sci* functional parameter distribution calculated for concrete surface number I.

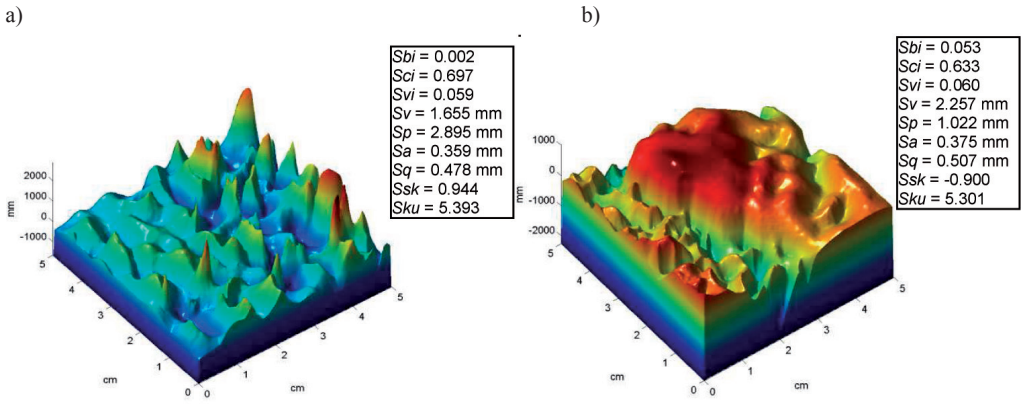

Fig. 12. Examples of the obtained surfaces topography images for a selected point E5: a) surface I; b) surface II.

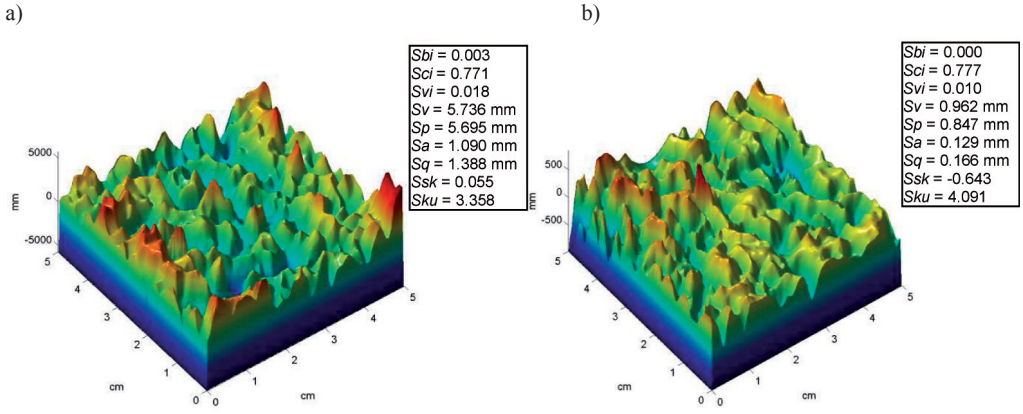

Fig. 13. Examples of the obtained surfaces topography images for a selected point F5: a) surface I; b) surface II.

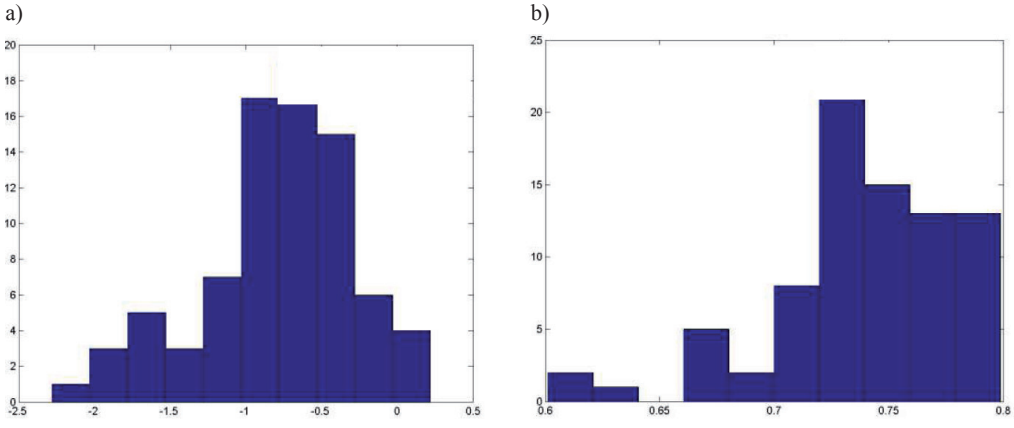

Fig. 14. a) The *Ssk* amplitude parameter distribution calculated for concrete surface II; b) the *Sci* amplitude parameter distribution calculated for concrete surface I.

Table 1 presents some values of the surface topography parameters for the analysed concrete slabs. Analysis of this values shows reduction of the average values of *Sq*, *Ssk* and *Svi* roughness parameters of surface I in comparison with the average values of the same parameters describing surface II. The average values of *Sku* and *Sbi* were observed to be higher for surface II while the values of parameter *Sci* are on a similar level for both surfaces.

Table 1. Values of some parameters of surface I and surface II.

SURFACE NO.	**I**	**II**	**I**	**II**	**I**	**II**
PARAMETERS	*Sq*		*Ssk*		*Sku*	
AVERAGE	0.30	0.70	−0.79	−0.01	4.42	4.08
DEVIATION	0.17	0.24	0.51	0.41	1.72	0.82
MAX. VALUE	1.04	1.54	0.22	0.94	11.64	7.30
MIN. VALUE	0.12	0.33	−2.28	−1.17	1.96	2.94
SURFACE NO.	I	II	I	II	I	II
PARAMETERS	*Sbi*		*Svi*		*Sci*	
AVERAGE	0.015	0.002	0.026	0.044	0.739	0.732
DEVIATION	0.019	0.002	0.018	0.033	0.041	0.036
MAX. VALUE	0.094	0.008	0.080	0.140	0.799	0.810
MIN. VALUE	0.000	0.000	0.002	0.004	0.601	0.629

After the analysis of the obtained parameters the question arose: which of the parameters show the largest differences? Therefore, the surface parameters obtained from surface I were divided by the surface parameters obtained from surface II (Table 2).

Table 2. Differences between the parameters of surface I and surface II.

SURFACE NO.	**I**	**II**	**I**	**II**	**I**	**II**
PARAMETERS	Sq1/Sq2		Ssk1/Ssk2		Sku1/Sku2	
AVERAGE	0.433	53.212	1.085	0.433	53.212	1.085
DEVIATION	0.693	1.241	2.095	0.693	1.241	2.095
MAX. VALUE	0.670	0.232	1.595	0.670	0.232	1.595
MIN. VALUE	0.347	1.954	0.688	0.347	1.954	0.688
SURFACE NO.	I	II	I	II	I	II
PARAMETERS	Sbi1/Sbi2		Svi1/Sv2		Sci1/Sci2	
AVERAGE	6.745	0.586	1.010	6.745	0.586	1.010
DEVIATION	11.922	0.563	1.153	11.922	0.563	1.153
MAX. VALUE	10.411	0.568	0.986	10.411	0.568	0.986
MIN. VALUE	−	0.426	0.955	−	0.426	0.955

The smallest differences were observed for the average value of the *Sci* parameter and the average value of the *Sku* parameter. The largest differences were found for the average value of the *Sbi* parameter and the average value of the *Ssk* parameter. It seems that the *Ssk* and *Sbi* parameters will be useful for analysing different concrete surface topographies. The *Ssk* parameter (skewness) for both analysed surfaces has a negative value which means that these

are surfaces with low peaks and deep valleys. The value of the difference for surface bearing index *Sbi* indicates greater adhesion at the interface in the case of the ground surface.

4. Conclusions and perspectives

Research on large area surface topography measurements and a methodology for measuring and analysing the surface topography of a concrete surface have been presented.

Two differently prepared concrete surfaces were examined. An advanced 3D scanner and the optical (digital light projection) method have been found to be particularly useful for the measurement of concrete surfaces.

TAS (*Topography Analysis and Simulation*) software has been developed for analysis of the topography of concrete surfaces. It enables data processing, calculation of parameters, data visualization and digital filtration.

The *Ssk* parameter (skewness) and bearing index *Sbi* were found to be useful for evaluation of properties of the examined concrete surfaces.

Two measurement strategies: simple and fast 3D scanning and partial scanning in selected areas corresponding to the device measurement space were applied and discussed.

The results of this research indicate that the direction towards developing a methodology of measuring the topography of concrete surfaces is proper. Further research will focus on a correlation between the pull-off adhesion and the concrete surface topography. Selecting the most relevant 3D roughness parameters for concrete surfaces still remains an open issue.

References

[1] Berkowski, P., Dmochowski, G., Grosel, J., Schabowicz, K., Wójcicki, Z. (2013). Analysis of failure conditions for a dynamically loaded composite floor system of an industrial building. *Journal of Civil Engineering and Management*, 19(4), 529–541.

[2] Farny, J. (2001). *Concrete floors on ground*. Portland Cement Association.

[3] Garbacz, A., Courard, L., Bissonnette, B. (2013). A surface engineering approach applicable to concrete repair engineering. *Bulletin of The Polish Academy of Sciences: Technical Sciences*, 61(1), 73–84.

[4] Courard, L., Lenaers, J., Michel, F., Garbacz, A. (2011). Saturation level of the superficial zone of concrete and adhesion of repair systems. *Construction and Building Materials*, 25(5), 2488–2494.

[5] Brown, C.A., Siegmann, S. (2001). Fundamental scales of adhesion and area-scale fractal analysis. *International Journal of Machine Tools and Manufacture*, 41(13), 1927−1933.

[6] Brown, C.A. (2001). Relating Surface Texture and Adhesion with Area-scale Fractal Analysis. *Tech XXIV, Sharing global pressure sensitive tape innovations, proceedings, a global conference*, Orlando, 49–58.

[7] Błaszczyński, T., Jasiczak, J., Ksit, B., Siewczyńska, M. (2006). Aspects of bond layer role in concrete repairs. *Archives of Civil and Mechanical Engineering*, 6(4), 73–85.

[8] Hola, J., Sadowski, L., Schabowicz, K. (2011). Nondestructive identification of delaminations in concrete floor toppings with acoustic methods. *Automation in Construction*, 20(7), 799–805.

[9] Tayeh, B., Abu Bakar, B., Megat Johari, M., Zeyad, A. (2014). Microstructural analysis of the adhesion mechanism between old concrete substrate and UHPFC. *Journal of Adhesion Science and Technology*, 28(18), 1846−1864.

[10] Hola, J., Schabowicz, K. (2010). State-of-the-art non-destructive methods for diagnostic testing of building structures – anticipated development trends. *Archives of Civil and Mechanical Engineering*, 10(3), 5−18.

[11] Sadowski, L. (2013). Non-destructive evaluation of the pull-off adhesion of concrete floor layers using RBF neural Network. *Journal of Civil Engineering and Management*, 19(4), 550–560.

[12] Sadowski, L., Hoła, J. (2014). New nondestructive way of identifying the values of pull-off adhesion between concrete layers in floors. *Journal of Civil Engineering and Management*, 20(4), 561–569.

[13] Królczyk, G.M., Nieslony, P., Królczyk, J.B., Samardzic, I., Legutko, S., Hloch, S., Barrans, S., Maruda, R.W. (2014). Influence of argon pollution on the weld Surface Morphology. *Measurement*, 70, 203−213.

[14] Królczyk, G., Raos, P., Legutko, S. (2014). Experimental analysis of surface roughness and surface texture of machined and fused deposition modelled parts. *Tehnički Vjesnik – Technical Gazette*, 21(1), 217−221.

[15] Siewczynska, M. (2008). *Effect of selected concrete parameters on adhesion of protective coatings*. PhD Thesis. Poznan University of Technology, Poznań.

[16] Garbacz A., Courard, L., Kostana, K. (2006). Characterization of concrete surface roughness and its relation to adhesion in repair systems. *Materials Characterization*, 56(4–5), 281–289.

[17] Davis, A. (2003). The non-destructive impulse response test in North America: 1985−2001. *NDT&E International*, 36, 185−193.

[18] Hertlein, B., Davis, A. (1996). Performance-based and condition-based NDT for predicting maintenance needs of concrete highways and airport pavements. *Nondestructive Evaluation of Aging Aircraft, Airports and Aerospace Hardware, Proceedings of SPIE 2945*, (1), 273−281.

[19] Franck, A., De Belie, N. (2008). Concrete floor-bovine claw contact pressures related to floor roughness and deformation of the claw. *Journal of Dairy Science*, 89(8), 2952−2964.

[20] Li, Z. (2011). *Advanced concrete technology*. John Wiley & Sons.

[21] Courard, L., Michel, F., Garbacz, A., Piotrowski, T. (2011). Surfology based concrete repair engineering. *European Symposium on Polymers in Sustainable Construction*, Warsaw.

[22] Czarnecki, S., Hoła, J., Sadowski, L. (2014). A non-destructive method of investigating the morphology of concrete surfaces by means of newly designed 3D scanner. *11th European Conference on Non-destructive Testing, Prague, Czech Republic*.

[23] Leach, R., Sherlock, B. (2014). Applications of super-resolution imaging in the field of surface topography measurement. *Surface Topography: Metrology and Properties*, 2(2), 023001.

[24] Mathia, T., Pawlus, P., Wieczorowski, M. (2011). Recent trends in surface metrology. *Wear*, 271(3–4), 494–508.

[25] Hocken, R., Chakraborty, N., Brown, C.A. Optical Metrology of Surfaces. *CIRP Annals – Manufacturing Technology*, 54(2), 169–183.

[26] Santos, P., Julio, E. (2013). A state-of-the-art review on roughness quantification methods for concrete surfaces. *Construction and Building Materials*, 38, 912–923.

[27] Stout, K., Sullivan, P., Dong, W., Mainsah, E., Luo, N., Mathia, T., Zahouani, H. (1993). The Development of Methods for the Characterisation of Roughness in Three Dimensions. *Commission of the European Communities*, Brussels-Luxembourg, Belgium.

[28] Deltombe, R., Kubiak, K., Bigerelle, M. (2014). How to select the most relevant 3D roughness parameters of a surface. *Scanning*, 36(1), 150−160.

[29] Thomas, T. (1999). *Rough Surfaces*. Imperial College Press.

[30] Sezen, H., Fisco, N. (2013). Evaluation and comparison of surface macrotexture and friction measurement methods. *Journal of Civil Engineering and Management*, 19(3), 387−399.

[31] Niemczewska-Wójcik, N., Mathia, T., Wójcik, A. (2014). Measurement Techniques Used for Analysis of the Geometric Structure of Machined Surfaces. *Management and Production Engineering Review*, 5(2), 27−32.

[32] Fisco, N., Sezen, H. (2013). Comparison of surface macrotexture measurement methods. *Journal of Civil Engineering and Management,* 19, S153−S160.

[33] Moreau, N., Roudet, C., Gentil, C. (2014). Study and Comparison of Surface Roughness Measurements. *Journees du Groupe de Travail en Modelisation Geometrique (GTMG'14)*, Lyon, France.

[34] Whitehouse, D. (2002). *Surfaces and Their Measurement*. Hermes Penton Science.

[35] Dzierwa, A., Reizer, R., Pawlus, P., Grabon, W. (2014). Variability of areal surface topography parameters due to the change in surface orientation to measurement direction. *Scanning*, 36(1), 170−183.

[36] Pawlus, P. (2005) *Surface topography: Measurement, analysis, influence*. Rzeszów University of Technology Press, Rzeszów.

[37] Ourahmoune, R., Salvia, M., Mathia, T., Mesrati, N. (2014). Surface morphology and wettability of sandblasted PEEK and its composites. *Scanning*, 36(1), 64–75.

[38] Grabon, W., Pawlus, P. (2014). Description of two-process surface topography. *Surface Topography: Metrology and Properties*, 2(2), 025007.

[39] Majchrowski, R. (2007). The influence of spiral sampling on surface topography parameters – simulation analysis. *Archives of Mechanical Technology and Automation*, 27(2), 71–80.

[40] Wieczorowski, M. (2001). Theoretical assumptions of spiral sampling application in surface topography measurement. *Archives of Mechanical Technology and Automation*, 21(2), 121−129.

[41] Myshkin, N., Grigoriev, Y., Chizhik, S., Choi, K., Petrokovets, M. (2003). Surface roughness and texture analysis in microscale. *Wear*, 254, 1001−1009.

[42] Wieczorowski, M., Ruciński, M., Koteras, R. (2010). Application of optical scanning for measurements of castings and cores. *Archives of Foundry Engineering*, 10, 265−268.

[43] Grzelka, M., Chajda, J., Budzik, G., Gessner, A., Wieczorowski, M., Staniek, R., Gapiński, B., Koteras, R., Krasicki, P., Marciniak, L. (2010). Optical coordinate scanners applied for the inspection of large scale housings produced in foundry technology. *Archives of Foundry Engineering*, 10, 255−260.

[44] Grzelka, M. (2008). Possible applications of the optical coordinate scanner GOM ATOS II. *Coordinate Measuring Technique, Problems and Implementations*, University of Bielsko-Biala, 45–52.

[45] Wieczorowski, M. (2006). Industrial application of optical scanner. *Zeszyty Naukowe Akademii Techniczno – Humanistycznej w Bielsku Białej*, 22, 381−390.